DOI: 10.15480/882.9329

Eighth International Symposium on Marine Propulsors
smp'24, Berlin, Germany, March 2024

Model tests of surface piercing propellers in open-water conditions

Jaeheon Kim[1], Shin Hyung Rhee[1,2+]

[1]Department of Naval Architecture and Ocean Engineering, Seoul National University, Seoul, Republic of Korea
[2]Research Institute of Marine Systems Engineering, Seoul National University, Seoul, Republic of Korea

ABSTRACT

Many high-speed planning vessels with speeds of 50 knots or higher adopt surface-piercing propellers that operate in partially submerged conditions with an air film formed on the propeller blade surfaces. Compared to conventional propellers, there is a lack of research on the performance of surface-piercing propellers. In this study, propeller open-water tests were conducted in a towing tank, considering the actual operating conditions. The test propeller used was the Modified Model-841-B, which was a modification of the Model-841-B propeller (Olofsson 1996). Thrusts, torques, and efficiencies were measured and calculated for two different surface-piercing propellers with different pitch ratios for various immersion ratios, shaft inclination angles, and Froude numbers. Propulsion performance and efficiency were evaluated for each condition. The effects of the operating conditions on the propeller performance were analyzed.

Keywords

Surface-piercing propeller, Propeller open-water test, Partially submerged condition, Ventilated cavity

1 INTRODUCTION

Recently demand for high-speed vessels has been increasing as unmanned warfare environments gain interest. Some of high-speed vessels adopt surface-piercing propellers for various reasons; for example, to avoid cavitation damage on the blades, to allow the large expanded area of the propeller, and to accommodate the small draft of the boat. A conventional screw propeller is operated in fully submerged conditions, whereas a surface-piercing propeller is mounted on the shaft at the transom stern and operated in inclined and partially submerged conditions. Due to such operating conditions, there is a lack of standardized test procedures and performance estimation methods for surface-piercing propellers.

There are only a few studies devoted to surface-piercing propellers available to the public. Olofsson (1996) performed tests on Model-841-B in the cavitation tunnel of KAMEWA AB. The tests were performed by varying the horizontal and vertical inclination angles, the revolution speed, and the advance ratio. The ventilated cavity generated during propeller operation was recorded. The effects of the Froude number and cavitation number on the propulsion coefficient were analyzed. Young and Kinnas (2004) analyzed some of Olofsson's test results using a three-dimensional boundary element method. The calculated blade load results were then compared with experimentally measured data, and the predicted ventilated pattern was validated against the experimental photographs.

Ferrando et al. (2007) conducted propeller open-water (POW) tests by varying the number of blades, pitch ratio, and immersion ratio of a surface-piercing propeller in a cavitation tunnel. Regression equations for thrust and torque coefficients in the partially ventilated regime were presented by analyzing the test results. Both the immersion ratio and pitch ratio were closely correlated with the thrust and torque coefficients.

Lorio (2010) conducted towing tank experiments to investigate the effects of immersion ratio and vertical and horizontal inclination angles on the propulsion performance of a commercial surface-piercing propeller with a high rake. When the immersion ratio increased, the change in the thrust coefficient was insignificant, but the torque coefficient increased. The thrust coefficient and efficiency decreased as the inclination angle increased, but the torque coefficient was nearly unchanged. Zhou et al. (2019) conducted POW tests of a six-blade surface-piercing propeller at different immersion ratios, while the number of rotations of the propeller was fixed. The six-component forces at the center of the propeller plane were obtained. As for the other study, the immersion ratio played the key role with close correlation with the thrust and torque coefficients. Kamran et al. (2022) investigated the effects of position parameters and Froude number on the performance of a surface-piercing propeller. The effects of the advance ratio and Froude number on the ventilated cavity generated during propeller operation were also analyzed. They reported that the thrust and torque coefficients decreased when the inclination angle exceeded a certain value.

Surface-piercing propeller blades in non-design conditions display a variety of interesting flow physics. Ha et al. (2023) studied air ventilation, thrust misalignment, and vortical flow structures of partially submerged propellers by conducting towing tank tests.

In this study, towing tank tests were conducted for open-water performance of two surface-piercing propellers. The propulsion performance measured was analyzed for various conditions of immersion ratio, inclination angle, pitch ratio, and Froude number.

2 Experimental setup and method

2.1 Surface-piercing propeller

Surface-piercing propellers are characterized by their wedge-shaped blade cross sections with a sharp leading edge and a blunt trailing edge. Such a wedge-shaped cross-section is called the super-cavitating blade section. Along the super-cavitating blade section, the ventilated cavity collapses behind the trailing edge, not on the blade surface, so the cavity behavior is relatively stable. A surface-piercing propeller's operating regimes are classified into fully ventilated regimes, transition regimes, and partially ventilated regimes based on the extent of the ventilated cavity, as shown in Figure 1.

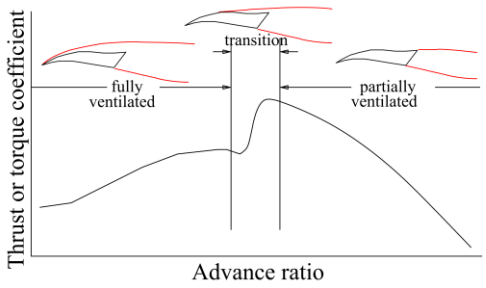

Figure 1 Tree major flow regimes for a surface-piercing propeller. Reproduced from figures presented in (Young and Kinnas 2004)

As the advance ratio increases, the operating regimes shift to the fully ventilated, transition, and then partially ventilated. The ventilated cavity around the propeller affects the propulsion performance significantly. The thrust and torque coefficients are low in the fully ventilated regime and increase sharply in the transition regime. In the partially ventilated regime, the thrust and torque coefficients decrease from their maximum values as the advance ratio increases.

2.2 Experimental geometry

The propeller geometry chosen for the present study is a Modified Model-841-B surface-piercing propeller. Its blade sections are slightly modified from Olofsson's (1996) Model-841-B to accommodate the manufacturing limitations of the computer numerical control machine available for the present study. Two propellers with different pitch ratios of 1.0 and 1.2 at the 0.7 radius were manufactured and used. Table 1 presents the principal particulars of Modified Model-841-B and Figure 2 shows its geometry.

Table 1 Principal particulars of Modified Model-841-B

Diameter	150 mm
Pitch at 0.7 radius	1.0, 1.2
Hub diameter	45 mm
Number of blades	4
Rotation direction	Right hand
Material	Aluminum
Surface finish	Red anodization

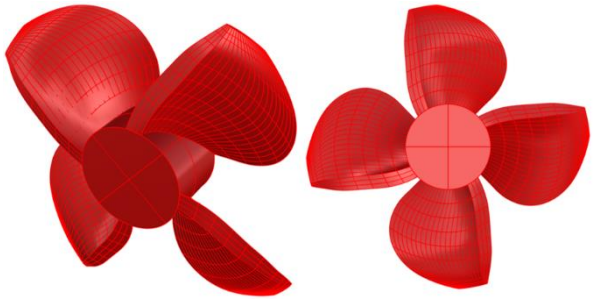

Figure 2 Geometry of Modified Model-841-B

2.3 Experimental facility and equipment

Experiments were conducted in the Seoul National University towing tank with a length of 110 m, breadth of 8 m, and depth of 3.5 m. Figure 3 shows a schematic diagram of the towing tank. The towing carriage, powered by AC servo motors, can reach a speed up to 5 m/s.

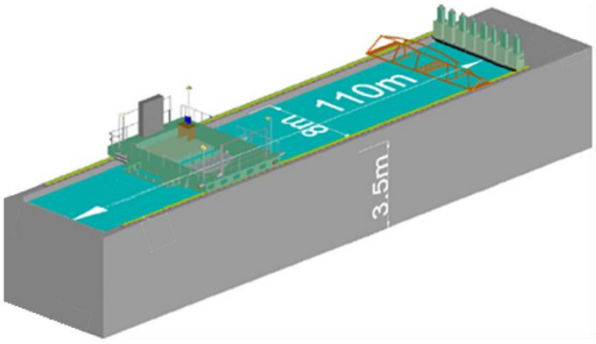

Figure 3 Seoul National University towing tank

A POW test dynamometer was used to measure thrust and torque. Measured data was transmitted in real time

to the data acquisition system on the towing carriage. A spray shield was installed to protect the equipment from spray generated during the propeller operation in partially submerged conditions. When adjusting the inclination angle, wedge-shaped supporting blocks were inserted between the POW dynamometer and the towing carriage mount. During the tests, a high-speed camera (Photron FASTCAM mini UX50-32GB model, outfitted with a Nikon AF-S NIKKOR 50 mm lens) was used to record the ventilated cavity. The recording was conducted at a rate of 2000 frames per second. Figure 4 shows the high speed filming system installed on the towing carriage.

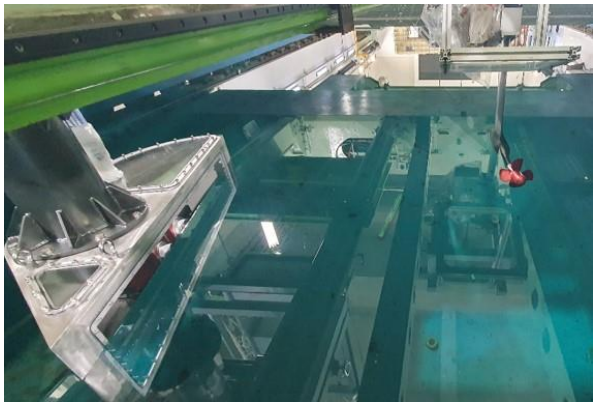

Figure 4 High speed filming system setup

2.4 Experimental conditions

The immersion ratio (I_T) was defined as Equation (1) where H is the immersion depth and D is the propeller diameter. Figure 5 illustrates the definition of I_T.

$$I_T = \frac{H}{D} \tag{1}$$

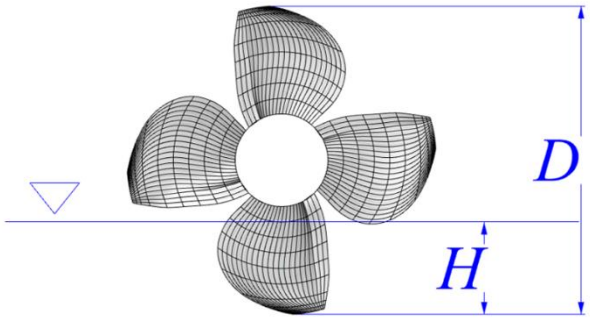

Figure 5 Definition of the immersion ratio (I_T)

The shaft inclination angle (γ) was defined as the angle from the horizontal axis, and the advance ratio (J) was defined as Equation (2), where V_A is the inflow velocity and n is the propeller revolutions per second (*rps*). Figure 6 shows the definition of γ.

$$J = \frac{V_A \cos(\gamma)}{nD} \tag{2}$$

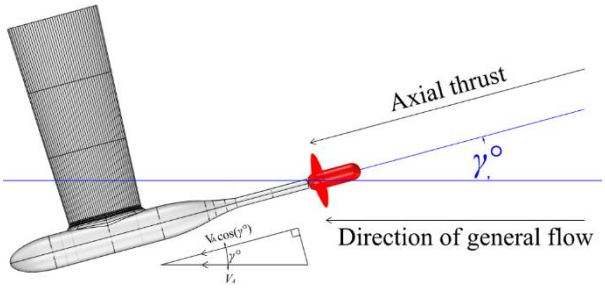

Figure 6 Definition of γ

Thrust coefficient (K_T), torque coefficient (K_Q), and efficiency (η_o) were defined as Equations (3), (4), and (5), respectively. T is the measured thrust, Q is the measured torque, and ρ is the density of water.

$$K_T = \frac{T}{\rho n^2 D^4} \tag{3}$$

$$K_Q = \frac{Q}{\rho n^2 D^5} \tag{4}$$

$$\eta_o = \frac{JK_T}{2\pi K_Q} \tag{5}$$

Froude number (Fr) was defined as Equation (6), where g is the gravitational acceleration.

$$Fr = \frac{revolution\ speed}{\sqrt{gD}} = \frac{nD}{\sqrt{gD}} \tag{6}$$

The experimental conditions, presented in Table 2, were set by varying the pitch ratio (P/D), γ, I_T, and Fr considering the operation conditions at sea.

Table 2 Test conditions

Variation	P/D	γ	I_T	Fr
Pitch ratio	1.0, 1.2	0°	0.3	2
Inclination angle	1.2	0°, 5°, 10°, 15°	0.3	2
Immersion ratio	1.2	0°	0.3, 0.5, 0.7	2
Froude number	1.2	0°	0.3	2, 3.5

3. Results and discussion

3.1 Effects of pitch ratio *P/D*

Figure 7 shows K_T, K_Q, and η_o at P/D = 1.0, 1.2. Figure 8 illustrates the projected area of the propeller blade according to P/D. Figure 9 shows changes in the ventilated cavity according to J at P/D = 1.0, 1.2.

P/D increase entailed the increase in the projected area of the propeller blade (Figure 8), which led to an increase in the volume of the ventilated cavity (Figure 9), because of the large air volume entrained from the free-surface. The increased volume of the ventilated cavity reduced the pressure difference between the suction and pressure sides and disrupted the incoming

flow to the propeller. This phenomenon was a contributing factor to the lower thrust observed in the fully ventilated regime, particularly as the *P/D* increased. As *J* increased and the flow regime became the transition one, the ventilated cavity started to collapse. In this regime, *P/D* increased with both K_T and K_Q. A change in *P/D* did not significantly affect K_Q at $J < 0.25$ though. In the fully ventilated regime, where the ventilated cavity covered the whole propeller blades, changes in *P/D* caused no dramatic effects on K_T and K_Q. The maximum η_o was higher with greater *P/D*. In the fully ventilated regime with a low *J*, both the pressure and suction sides were surrounded by a ventilated cavity, causing a small pressure difference and a low K_T. As the size of the suction side ventilated cavity decreased in the transition regime, the increased pressure difference resulted in the greater K_T.

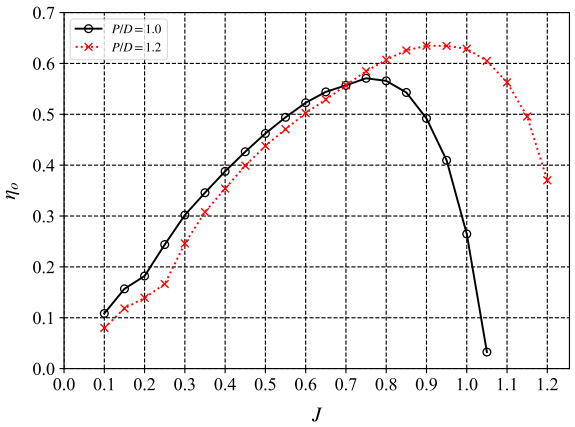

Figure 7 K_T, K_Q, η_o while varying *P/D* = 1.0, 1.2
[γ = 0°, I_T = 0.3, *Fr* = 2]

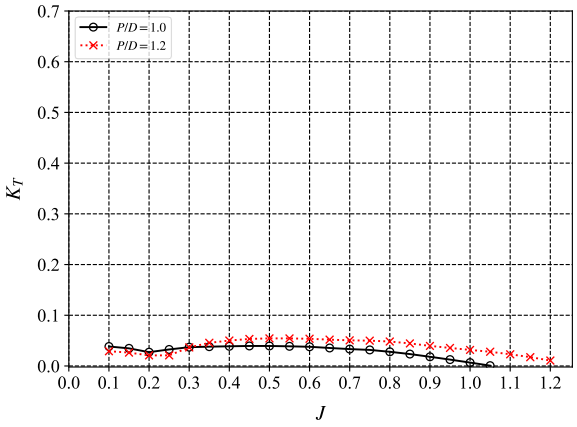

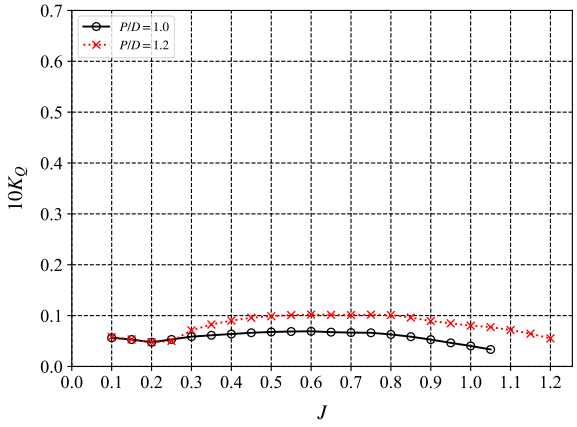

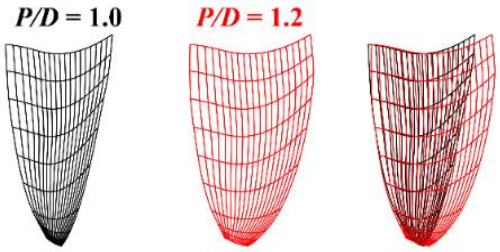

Figure 8 Projected blade area

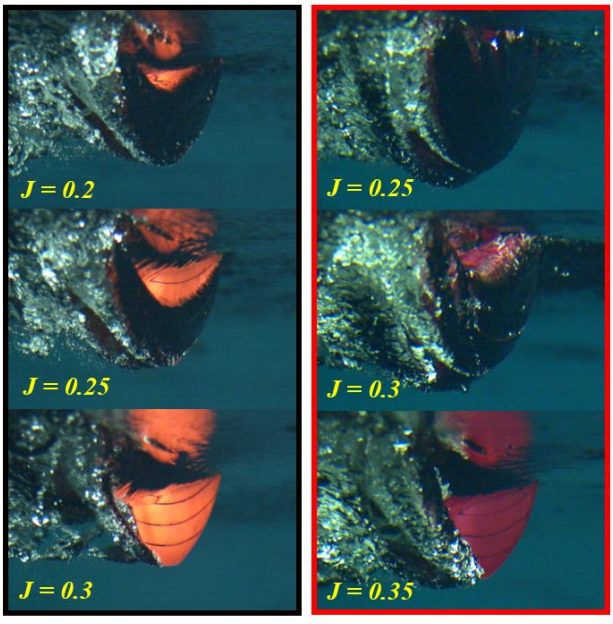

<*P/D* = 1.0> **<*P/D* = 1.2>**

Figure 9 Changes in the ventilated cavity according to *J* at *P/D* = 1.0, 1.2

3.2 Effects of shaft inclination angle γ

Figure 10 shows K_T, K_Q, and η_o with varying γ. K_T decreased as γ increased in the fully ventilated and transition regime at $J < 0.4$. In the partially ventilated regime at $J \geq 0.55$, K_T increased with γ, except for γ of 5 °. K_Q showed no significant correlation with variations in γ in the fully ventilated and transition regimes at $J < 0.4$. In the partially ventilated regime at $J > 0.55$, K_Q increased with γ. Similar to the cases of P/D variation, at low J, the propeller operated inside the ventilated cavity, and γ had little influence on K_Q. η_o decreased as γ increased in all regimes. Figure 11 shows the effects of γ on the ventilated cavity. As γ increased, the ventilated cavity collapsed at higher J, because the propeller rotated closer to the free surface as γ increased, resulting in an increased ventilated cavity volume. This increased volume caused a reduction of thrust, leading to a decreased η_o.

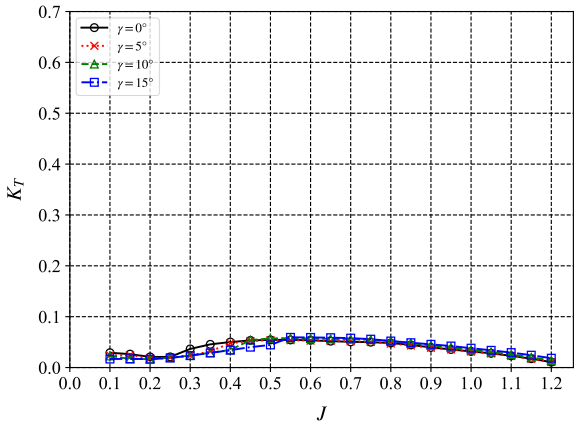

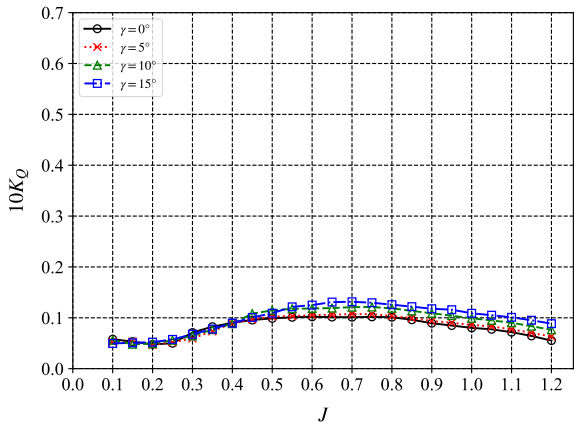

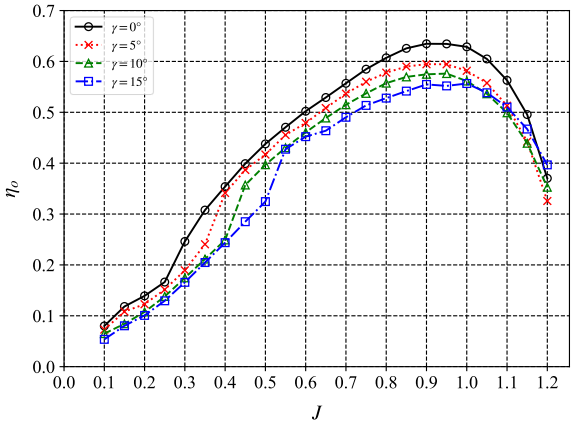

Figure 10 K_T, K_Q, η_o while varying γ = 0°, 5°, 10°, 15° [P/D = 1.2, I_T = 0.3, Fr = 2]

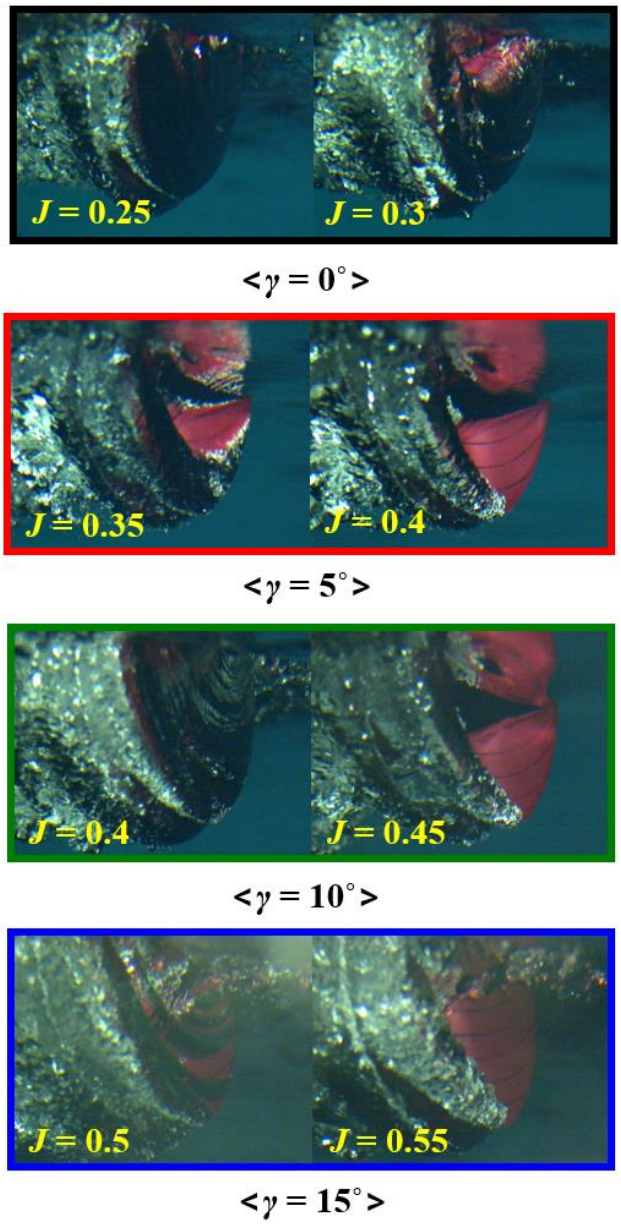

Figure 11 Effect of γ on the ventilated cavity

3.3 Effects of immersion ratio I_T

K_T, K_Q, and η_o at different I_T are shown in Figure 12. As I_T increased, all regimes' K_T and K_Q increased noticeably. As I_T increased, K_T and K_Q increased rapidly at J = 0.2 - 0.5. The effect of I_T on K_T and K_Q was relatively small in the fully ventilated regime due to the cushion effect of ventilated cavity. At $J < 0.4$, in the fully ventilated and some transition regimes, the effect of I_T on η_o was insignificant. At $J \geq 0.4$, η_o was the highest at I_T of 0.3. At I_T of 0.5 and 0.7, the propeller shaft was submerged together with the propeller and did not contribute to thrust generation at all. η_o at I_T of 0.5 and 0.7 was lower than that at I_T of 0.3 as a result. In Figure 13, I_T of 0.5 and 0.7 showed air inflow near the propeller boss cap. Air inflow near the propeller boss cap affected the formation of the propeller ventilated cavity.

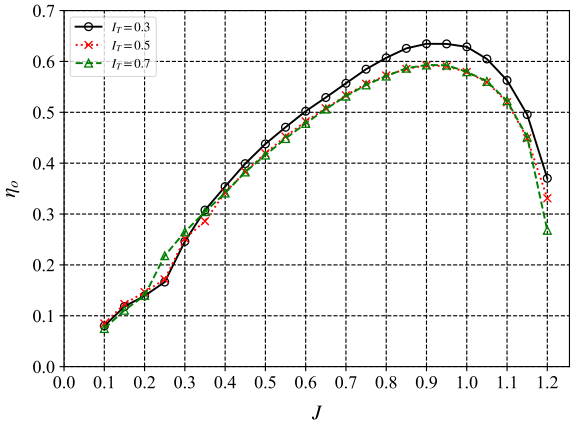

Figure 12 K_T, K_Q, η_o while varying I_T = 0.3, 0.5, 0.7 [P/D = 1.2, γ = 0, Fr = 2]

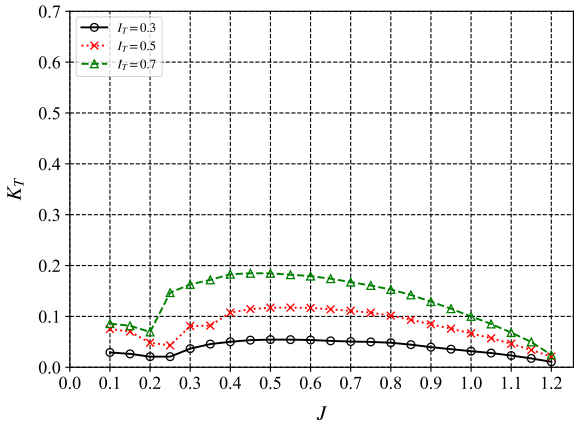

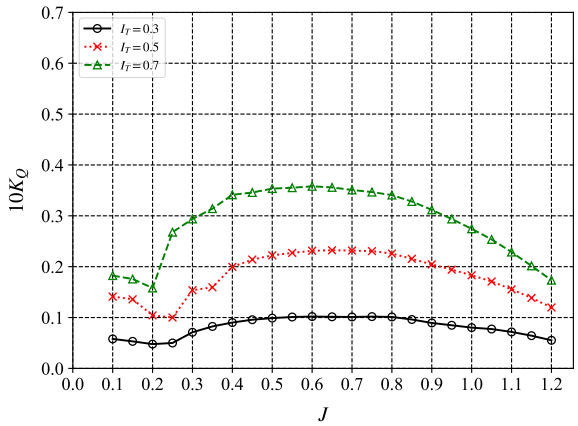

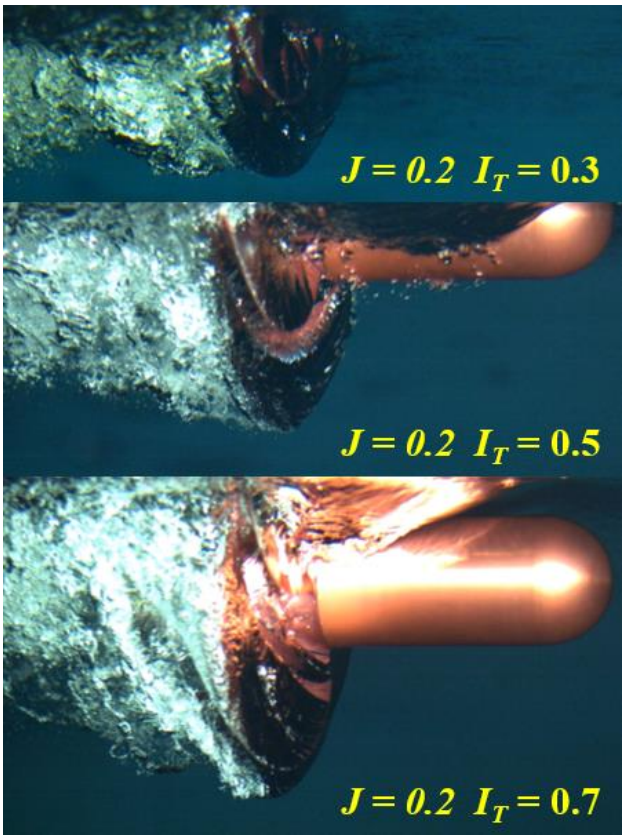

Figure 13 Photographs of air entrainment above the propeller boss cap

3.4 Effects of Froude number Fr

Figure 14 shows K_T, K_Q, and η_o at Fr = 2 and 3.5. Figure 15 shows the effect of Fr on the ventilated cavity. At $J < 0.25$, the results at Fr of 2 showed a tendency for K_T and K_Q to decrease, but the results at Fr of 3.5 showed a tendency to increase gradually. At higher Fr, the volume of the ventilated cavity was larger, and thereby the increased cavity volume disrupted the flow entering the propeller. This disturbance led to a decrease in both K_T and K_Q in both the fully ventilated and transition

regimes. The transition regime of Fr of 3.5 occurred at a higher J than the transition regime of Fr of 2, because of the increased ventilated cavity volume. In the fully ventilated regime at a low J, the effect of Fr on η_o was insignificant. In the transition regime, η_o was higher at lower Fr. This was due to the formation of a larger ventilated cavity around the propeller at higher Fr. In the partially ventilated regime with $J \geq 0.6$, η_o increased with Fr.

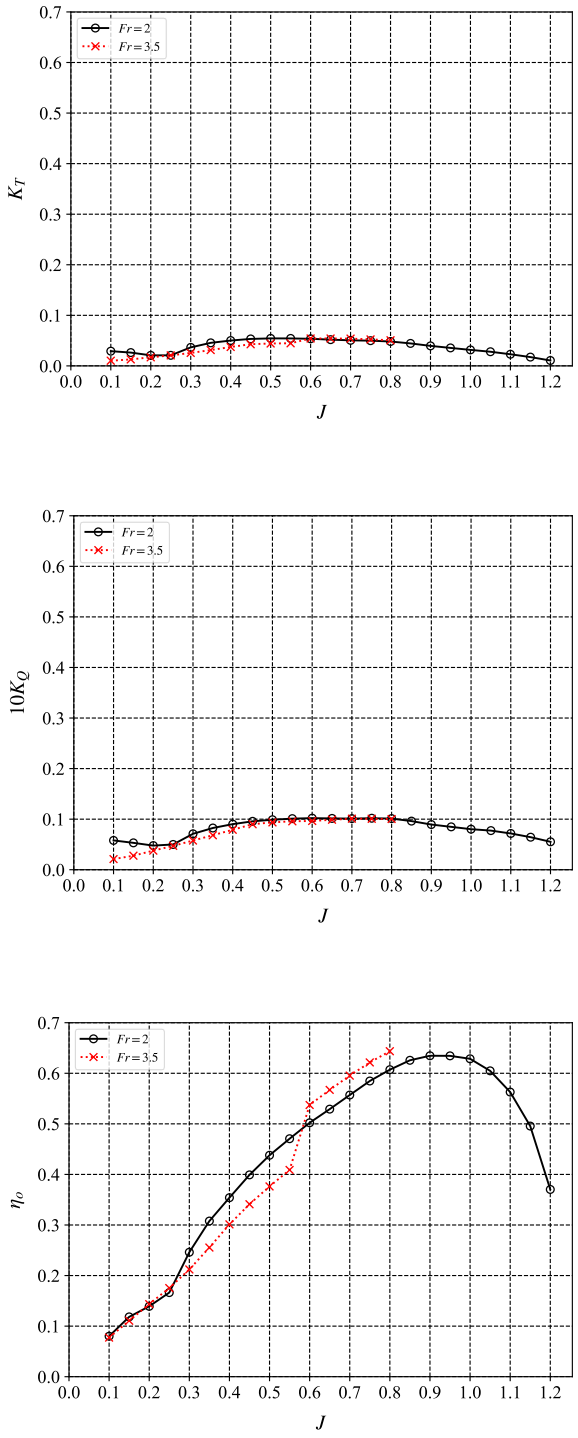

Figure 14 K_T, K_Q, η_o while varying Fr = 2, 3.5 [P/D = 1.2, γ = 0, I_T = 0.3]

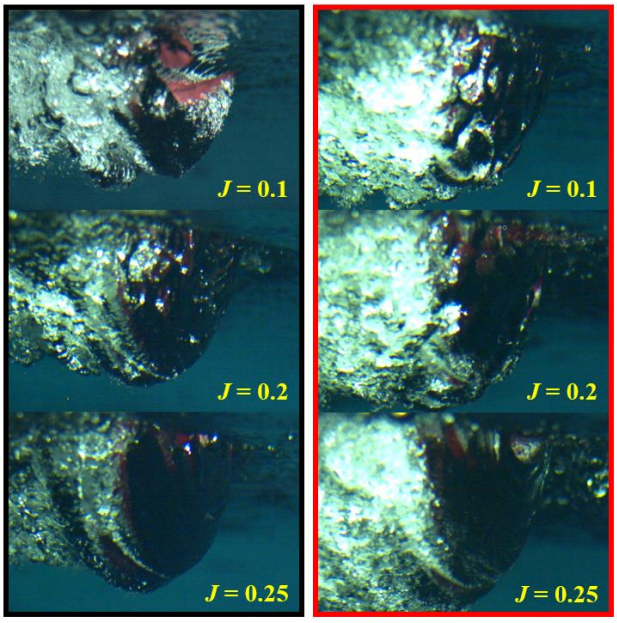

Figure 15 Effect of Fr on the ventilated cavity at the fully ventilated regime

4. Conclusions

POW tests were conducted for two surface-piercing propellers, considering actual operating conditions. Various P/D, γ, I_T, and Fr were tested to analyze the effects of each condition on the propeller's performance.

In the partially ventilated regime, η_o increased with P/D. In the fully ventilated regime, the effects of P/D on K_Q were insignificant, while K_T decreased as P/D increased. As P/D increased, the volume of the ventilated cavity expanded, leading to thrust loss and disturbing the flow entering the propeller.

As γ increased, K_T decreased in the fully ventilated and transition regimes, but increased in the partially ventilated regime. The increase in γ caused the propeller blade to rotate closer to the free surface, promoting the formation of a ventilated cavity. As γ increased, η_o decreased in all the regimes.

As I_T increased, both K_T and K_Q increased significantly in all the regimes. The propeller boss cap was positioned at the free surface when I_T = 0.5, and submerged below the free surface when I_T = 0.7. Additional air entrainment near the propeller boss cap occurred due to interaction with the free surface and enhanced the formation of the ventilated cavity, resulting in a change in the multi-phase flow structure.

At higher Fr, the volume of the ventilated cavity increased due to increased rotational speed. The increased cavity volume at a higher Fr led to a shift to the partially ventilated regime at a higher J. In the fully ventilated regime, where the ventilated cavity had a significant effect, lower Fr led to higher K_T. On the other

hand, in the partially ventilated regime, as the volume of the ventilated cavity decreased, K_T increased with Fr.

I_T had the most significant influence on both K_T and K_Q. Compared to previous studies, a common tendency was confirmed that K_Q increased as I_T and P/D increased.

In the present study, it was learned that for efficient operation of a surface-piercing propeller, operating at low I_T with a large P/D and a smaller γ, i.e., as parallel as possible to the water surface, is desirable.

REFERENCES

Ferrando, M., Crotti, S., & Viviani, M. (2007). 'Performance of a family of surface piercing propellers'. Proceedings of the 2nd International Conference on Marine Research and Transportation, Ischia, Italy.

Ha, J., Park, J., Park, G., Kim, J., Kim, J., Seo, J. & Rhee, S. H. (2023). 'Experimental study on the propulsion performance of a partially submerged propeller'., International Journal of Naval Architecture and Ocean Engineering, **15**, 100516.

Kamran, M., Nouri, N.M., Goudarzi, H., & Golrokhifar, S. (2022). 'Experimental evaluation of the effect of positioning and operating parameters on the performance of a surface-piercing propeller'. Scientific Reports **12. 1.**

Lorio, J. M. (2010). Open water testing of a surface piercing propeller with varying submergence, yaw angle and inclination angle., Florida Atlantic University, Boca Raton, Florida.

Olofsson, N. (1996). Force and flow characteristics of partially submerged propeller., Doctoral Thesis, Chalmers University of Technology, Göteborg, Sweden.

Young, Y. L. & Kinnas, S. A. (2004). 'Performance prediction of surface-piercing propellers'., Journal of Ship Research, **48(4)**, 288-304.

Zhou, J., Lu, L-Z., Rui, W. & Zhai, S-C. (2019). 'Experimental study of six-component forces on surface piercing propeller in uniform flow'. Proceedings 16th Symposium on Marine Propulsors, Rome, Italy.